

Effect of Incorporating Bis(2-hydroxyethyl) Terephthalate on Thermal and Mechanical Properties and Degradability of Poly(butylene succinate)

Hadi Shirali¹, Mehdi Rafizadeh^{*2}, and Faramarz Afshar Taromi³

¹Department of Polymer Engineering and Color Technology, Amirkabir University of Technology, Iran

²Corresponding author, Department of Polymer Engineering and Color Technology, Amirkabir University of Technology, PO Box 15875-441, Tehran, Iran

³Department of Polymer Engineering and Color Technology, Amirkabir University of Technology, Iran

Received March 16, 2015; Revised May 4, 2015; Accepted May 16, 2015

Abstract: A series of novel random copolymers of poly(butylene succinate-co-ethylene terephthalate) were synthesized and characterized in terms of thermal and mechanical properties, crystallinity and biodegradability. The composition and microstructure of the prepared copolyesters were characterized by ¹H NMR and ¹³C NMR, respectively. It was seen that the PBS sequence length decreases with ethylene terephthalate content. All copolymers are semi-crystalline and crystallinity and crystallite size decrease slightly with the comonomer content up to 10%, but the introduction of 20% comonomer leads to decrease the crystallinity up to 29%. The melting temperature of copolyesters decreases with the comonomer content according to the Baur's equation that indicates only PBS blocks crystallize and crystallite size is decreased with the comonomer content. It was also investigated that the elastic modulus also decreases slightly with the comonomer content. However, the elongation at break increases by 500% due to the decrease in crystallite size and crystallinity. Incorporating non-biodegradable aromatic comonomer has a little effect on copolyester degradability because of the randomness and lower crystallite size.

Keywords: copolyester, poly(butylene succinate), bis(2-hydroxyethyl) terephthalate, degradability, crystallization.

Introduction

Recently, reducing the amount of polymer wastes, due to their long-lasting behavior in the environment, have been attracted a great deal of attention.¹ Hence, researchers have focused on developing new biodegradable materials with a predetermined degradation time.^{2,3} Natural and synthetic polyesters are the most investigated biodegradable polymers that could be classified into different groups based on the kind of their repeated unit: poly(hydroxyacid)s, poly(hydroxyalkanoate)s and poly(alkylene dicarboxylate)s.⁴ Poly(ϵ -caprolactone) (PCL), poly(L-lactic acid) (PLLA), poly(3-hydroxybutyrate) (PHB), and poly(butylene succinate) (PBS) are the most important synthetic biodegradable aliphatic polyesters.⁵⁻⁷ However, their physical and mechanical properties limit their applications. Nowadays, polyethylene and polypropylene have been substituted with PBS in many fields due to its considerable properties such as relatively high thermal and mechanical stability, biodegradability, relatively high melting point, and good processability.⁸ One draw-back is the difficulty in reaching the high molecular weights. It is difficult to prepare high-molecular-weight PBS *via* two-steps polymer-

ization process because of the thermal decomposition at the high reaction temperatures.⁹ As the molecular weight increases, the mechanical properties are improved. Moreover, biodegradation rate of PBS is affected by crystallinity and decreases with crystallinity percent and crystallite size. Hence, improving PBS properties and extending its applications is challenging and interesting tasks. Contrary to the aliphatic polyesters, aromatic polyesters such as poly(ethylene terephthalate) (PET) are not biodegradable under the common environment but they possess low cost and high physical properties. Therefore, Copolymerization of aliphatic and aromatic polyesters is an approach to obtain a polymer with the desired properties. Several aliphatic-aromatic copolyesters have been synthesized so far. Munoz-Guerra *et al.*¹⁰ prepared poly(butylene succinate-*b*-ethylene terephthalate) copolyester using reactive blending. Hydrolysis was found to occur mainly in the aliphatic ester groups and increasing terephthalic groups to PBS lead to the decrease in hydrolysability up to 55%. Further investigations in Munoz works revealed that the elasticity modulus and tensile strength decrease with the content of PBS, whereas the elongation at break considerably increases, simultaneously. However, not any considerable differences were reported regarding tensile properties for the copolyesters prepared at different melt-mixing times. Galeski *et al.*¹¹ also synthesized

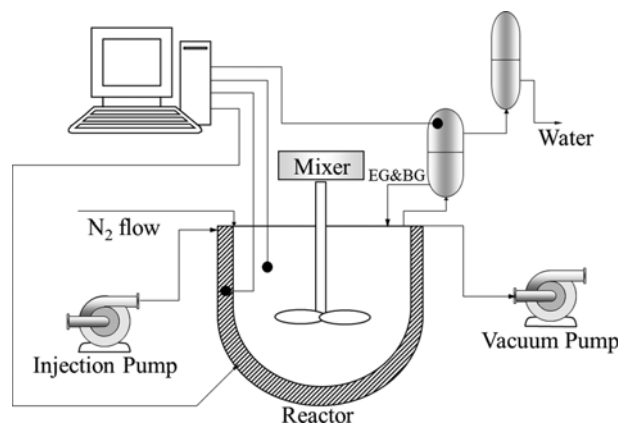
*Corresponding Author. E-mail: mehdi@aut.ac.ir

new type of biodegradable copolyester named poly(butylene adipate-*co*-succinate-*co*-glutarate-*co*-terephthalate) (PBASGT). Their investigations showed that incorporating aliphatic units in the polymer leads to decreasing the degree of crystallinity following a remarkable decrease in the melting temperature in comparison to PBT. The sequence distribution of the comonomers reveals that the copolyester is more or less random however, it is still crystallizable. Piorkowska *et al.*¹² measured the mechanical properties of melt mixed of PLA with 25-35 wt% of PBASGT. They showed that this polymer has the ultimate strain 20 times larger and the tensile impact strength 2.5 times larger than neat PLA.

In this work, a new random copolyester, poly(butylene succinate-*co*-ethylene terephthalate) (PBSET), was synthesized and its properties were evaluated. First, the esterification process of ethylene glycol with terephthalic acid and butylene glycol with succinic acid was performed, separately. PBSET was prepared *via* polycondensation of two resulted monomers of bis(2-hydroxybutyl) succinate (BHBS) and bis(2-hydroxyethyl) terephthalate (BHET). The effect of molecular structure and thermal properties were investigated on the mechanical properties and degradability. It was expected that PBSET copolyester at a certain composition would have better thermal and mechanical properties, such as higher melting point, modulus of elasticity and elongation at break than PBS due to the incorporation of prepolymer PET into the copolyesters. The biodegradability of the copolyesters is also tested in NaOH solution.

Experimental

Materials. Ethylene glycol (EG) and terephthalic acid (TA) were supplied by Shahid Toundgoyan Petrochemical Complex, Mahshar, Iran. Succinic acid (SA), butylene glycol (BG), titanium butoxide (TBT), as polycondensation catalyst, and highly pure chloroform, as solvent for intrinsic viscosity measurement, were bought from Merck Co., Darmstadt, Germany.



Scheme I. Schematic view of used setup.

Setup. A homemade laboratory-scale reactor was used to prepare PBS and its copolyesters. Scheme I shows a schematic of the setup. The reactor is heated using an electrical heater, isolated using a ceramic-type cover and cooled by airflow when needed. A nitrogen flow was used to maintain the required pressure. Moreover, nitrogen passes through an electrical condenser to separate synthesized water and alcohol during esterification step. A vacuum pump is used to apply vacuum and separate side product in polycondensation.

Synthesis of Copolyesters. For the preparation of BHBS, SA and BG were mixed with alcohol to acid molar ratio of 1.7 and poured into the reactor. The paste was mixed for 30 min at 140 °C under 3.5 bars. Consequently, the temperature was increased to 210 °C. As soon as the temperature reached 210 °C, the esterification step started and continued until no more water was collected (about 105 min). Water vapor was cooled, gathered, and weighed on a regular basis (every 15 min) as an indication of reaction extent.

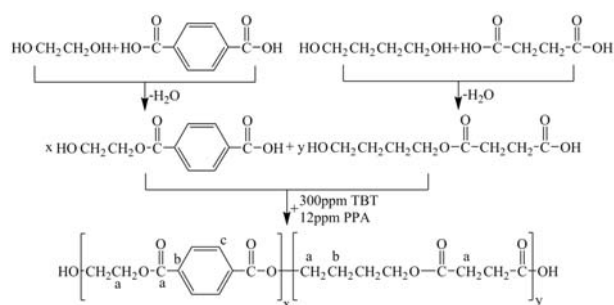
For the preparation of BHET, the synthesis route of BHET is the same as BHBS, but paste mixing and esterification temperatures are 200 and 245 °C, respectively.

For preparation of PBSET, BHBS and BHET monomers, TBT as catalyst and PPA as thermal stabilizer were mixed in the reactor for 10 min at 200 °C and 2 bars. Consequently, the temperature was increased to 250 °C and vacuum was applied. Polycondensation step started and continued for an hour as the temperature reached 250 °C, temperature then was raised to 265 °C and polymerization stopped after mixer torque reached the desired value. Scheme II describes the synthesis mechanism of the copolyesters.

Characterization. OC type Ubbelohde was used to measure the intrinsic viscosity of samples at 25±0.1 °C. Chloroform was used as the solvent. The number average molecular weight of samples was approximated using the following equation:⁸

$$\bar{M}_n = 3.29 \times [\eta]^{1.54} \quad (1)$$

Infrared spectra were recorded on a Nexus 670 spectrophotometer from Nicolet Co. (Waltham, MA) at room temperature. The samples were prepared as films or pellet by mixing 1 mg with 100 mg of KBr.



Scheme II. Reactions of PBSET copolyesters preparation.

^1H NMR and ^{13}C NMR spectra were recorded on a Bruker Avance (Switzerland) 400. CDCl_3 was used as the solvent and lock the spectrometer and tetramethylsilane (TMS) as reference, respectively. Spectrometer was operated at 400 MHz and 25 °C.

Thermal and Mechanical Properties. DSC tests were performed on a Mettler-Toledo (Columbus, OH) 822e instrument and Indium was used to calibrate the instrument. Sample (5–8 mg) was heated to remove the thermal history, then cooled down, then heated again up to 270 °C. The rate of heating and cooling was 10 °C/min and the samples were heated from -50 °C to obtain DSC thermograms.

Spherulite Morphology of copolyesters was examined on a Leica model DMRX Linkam England polarized optical microscope. Samples were sandwiched between two glass plates and heated to 200 °C for 2 min to complete melting of crystallites and cooled to the room temperature.

XRD pattern were recorded using a EQuinox 3000 model (tube voltage: 40 kV and tube current: 30 mA) with a $\text{CuK}_{\alpha 1}$ irradiation ($\lambda=0.1541874$ nm). Samples were scanned in the fixed-time mode for 2θ equals 4° to 120°. The samples were hot pressed to produce films with dimension of 20×20×0.1 mm at 120 °C and cooled to room temperature with the rate of 5 °C/min.

Dynamic mechanical thermal analysis (DMTA) was performed using compression molded samples (45×15×3 mm³) and TA Instrument, model DMA983, in tensile mode. Temperature sweep was carried out from -50 to 150 °C at 1 HTz with heating rate of 5 °C/min.

Tensile properties of the copolymers were tested on specimens prepared by hot pressing at a crosshead speed of 50 mm·min⁻¹ at the room temperature.

Degradability. Hydrolytic degradation of the copolyesters was evaluated using 1 M NaOH aqueous solution. The samples were hot pressed to films with dimension of 10×10×0.1

mm and weight of W_0 . 1 M of NaOH aqueous solution was then poured into a glass container at 37 °C and the films were added to it. After the predetermined time, the samples were taken out of the container and washed with demineralized water for three times, then were dried at 40 °C in a vacuum oven to reach a constant weight (W_1). The weight loss of the sample, as degradation rate, was calculated using the following equation:

$$W_{loss} = \frac{W_0 - W_1}{W_0} \times 100 \quad (2)$$

Results and Discussion

PBS and PBSET copolyesters with different percentages of BHET were synthesized as described in the experimental part. The characteristics of the synthesized copolyesters are shown in Table I. The number next to the PBSET stands for the mole percentage of BHET. Intrinsic viscosity and number average molecular weight of the product were between of 1.17–1.64 dL/g and 42,000–71,000 g/mol, respectively.

An FTIR spectrum of PBSET10 is shown in Figure 1. The sharp peak at 1721 cm⁻¹ is corresponded to C=O carbonyl group in ester band. Two sharp peaks at 1101 and 1260 cm⁻¹ are also related to the aromatic and aliphatic C-O bond in the ester group, respectively. These peaks demonstrate that the sample is copolyester. Broad peak at 3429 cm⁻¹ corresponds to the OH

Table I. Characteristic of Synthesized PBS and Its Copolyesters

Sample	BHET/BHBS	COOH	$[\eta]$ (g/dL)	M_n (g/mol)
PBS	0/100	17	1.64	71,000
PBSET5	5/95	29	1.2	43,600
PBSET10	10/90	31	1.22	44,900
PBSET20	20/80	31	1.17	41,800

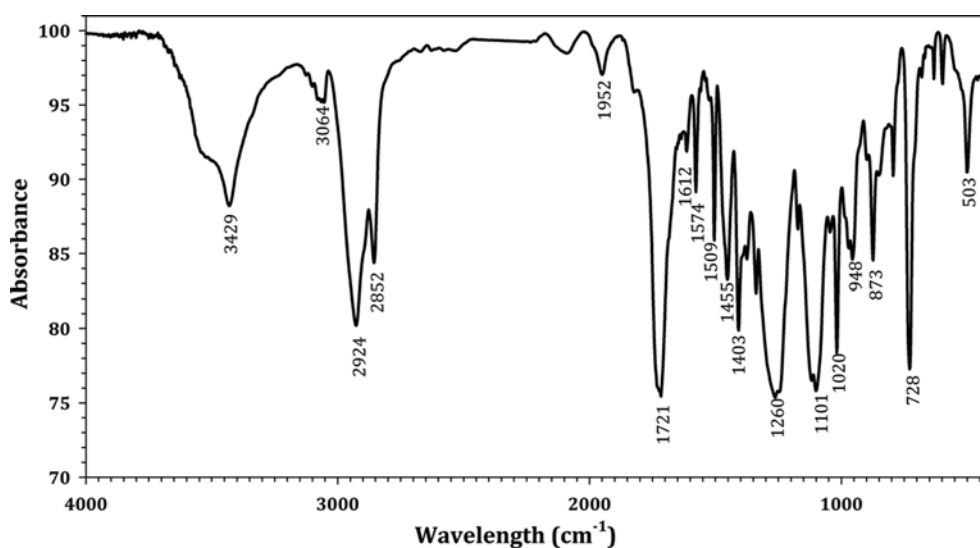


Figure 1. Infrared spectra of PBSET10.

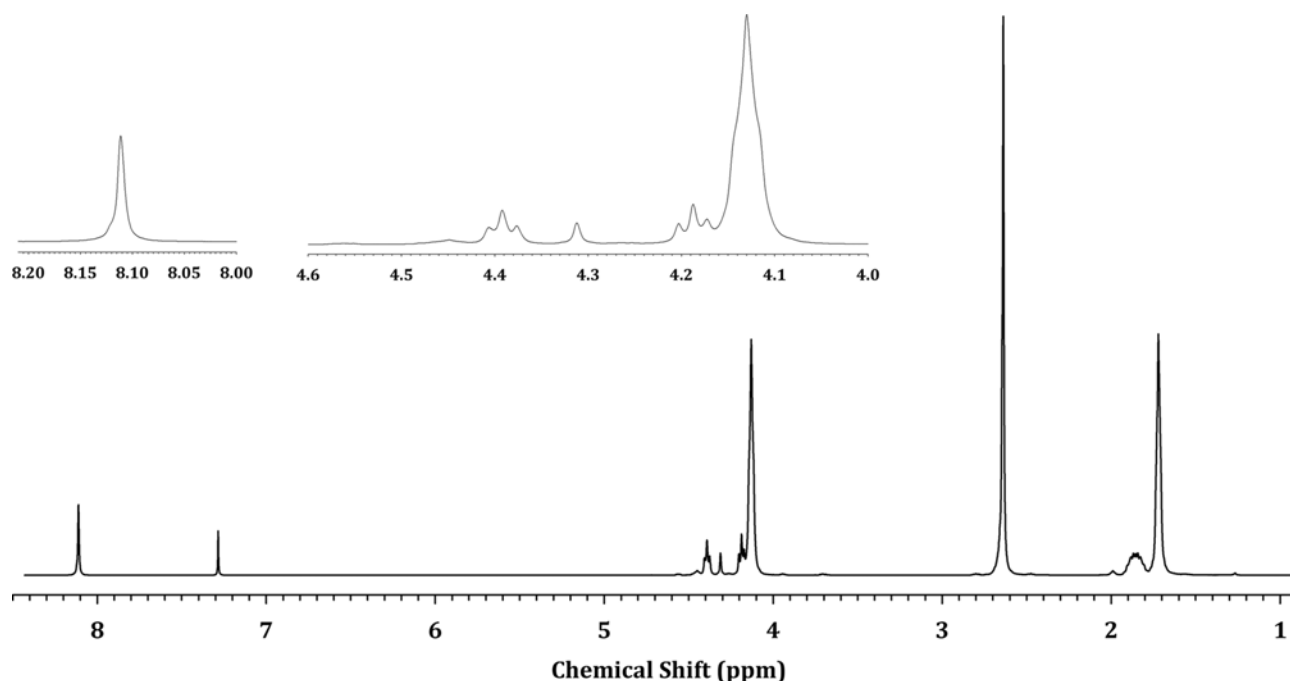


Figure 2. ^1H NMR spectrum of PBSET10.

stretching vibrations of structural hydroxyls and Absorbed water. Peaks at 2924 and 2852 cm^{-1} are attributed to the asymmetric and symmetric stretching vibrations of methylene groups. The out of plane C-H bending and C-H stretching of aromatic ring could be found from two peaks at 728 and 3025 cm^{-1} , respectively.¹³⁻¹⁵ There is a good agreement between the spectra for all the copolyesters.

^1H NMR spectrum of PBSET10 is shown in Figure 2. Assignments for shifts are: $^E\text{H}_a$ (4.84 ppm), $^T\text{H}_c$ (8.16 ppm), $^B\text{H}_a$ (4.13 ppm), $^B\text{H}_b$ (1.77 ppm), and $^S\text{H}_a$ (2.65 ppm),^{9,16-18} which ^EH , ^BH , ^SH , and ^TH show hydrogen of EG, BG, SA, and TPA, respectively. Subscripts are shown in the Scheme II. BG:EG and TPA/SA molar ratio in polymer chains were calculated according to the following equations:

$$\text{BG/EG} = \frac{^E\text{H}_a}{(^E\text{H}_a + ^B\text{H}_a)} \quad (3)$$

$$\text{TPA/SA} = \frac{^T\text{H}_c}{(^T\text{H}_c + ^S\text{H}_a)} \quad (4)$$

The degree of randomness, mean length of sequences, and dyad sequence distribution could also be estimated using the ^1H NMR spectra. There are eight signals that are related to methylene group of EG and BG groups, which is named "a" in Scheme II terephthalate ethylene succinate, TES, at 4.392 ppm, terephthalate ethylene terephthalate, TET, at 4.406 ppm, succinate ethylene succinate, SES, at 4.312 ppm, succinate ethylene terephthalate, SET, at 4.376 ppm, terephthalate butylene succinate, TBS, at 4.187 ppm, terephthalate butylene terephthalate, TBT, at 4.203 ppm, succinate butylene succinate, SBS, at 4.130 ppm and succinate butylene terephthalate, SBT, at 4.172 ppm. The degree of randomness could be

estimated using the areas under these eight peaks, defined as f_{TES} , f_{TET} , f_{SES} , f_{SET} , f_{TBS} , f_{SBT} , f_{SBS} , and f_{TBT} , respectively. First, the molar ratios of ethylene terephthalate groups, P_{ET} , butylene terephthalate groups, P_{BT} , ethylene succinate groups, P_{ES} , and butylene succinate groups, P_{BS} , are calculated *via* the following equations:

$$P_{ET} = (f_{TES} + f_{SET})/2 + f_{TET} \quad (5)$$

$$P_{BT} = (f_{TBS} + f_{SBT})/2 + f_{TBT} \quad (6)$$

$$P_{ES} = (f_{TES} + f_{SET})/2 + f_{SES} \quad (7)$$

$$P_{BS} = (f_{TBS} + f_{SBT})/2 + f_{SBS} \quad (8)$$

The number-average sequence length of ET, BT, ES, and BS units (L_{nET} , L_{nES} , L_{nBT} , and L_{nBS} , respectively) are obtained using the following equations:

$$L_{nET} = 2P_{ET}/(f_{TES} + f_{SET}) \quad (9)$$

$$L_{nES} = 2P_{ES}/(f_{TES} + f_{SET}) \quad (10)$$

$$L_{nBS} = 2P_{BS}/(f_{TBS} + f_{SBT}) \quad (11)$$

$$L_{nBT} = 2P_{BT}/(f_{TBS} + f_{SBT}) \quad (12)$$

Finally, the degree of randomness (R) is calculated from:

$$R = 1/L_{nAr} + 1/L_{nAI} = 2/(L_{nBT} + L_{nET}) + 2/(L_{nBS} + L_{nES}) \quad (13)$$

If the value of R is close to 1.0, random copolyester is produced. The results are shown in Table II.

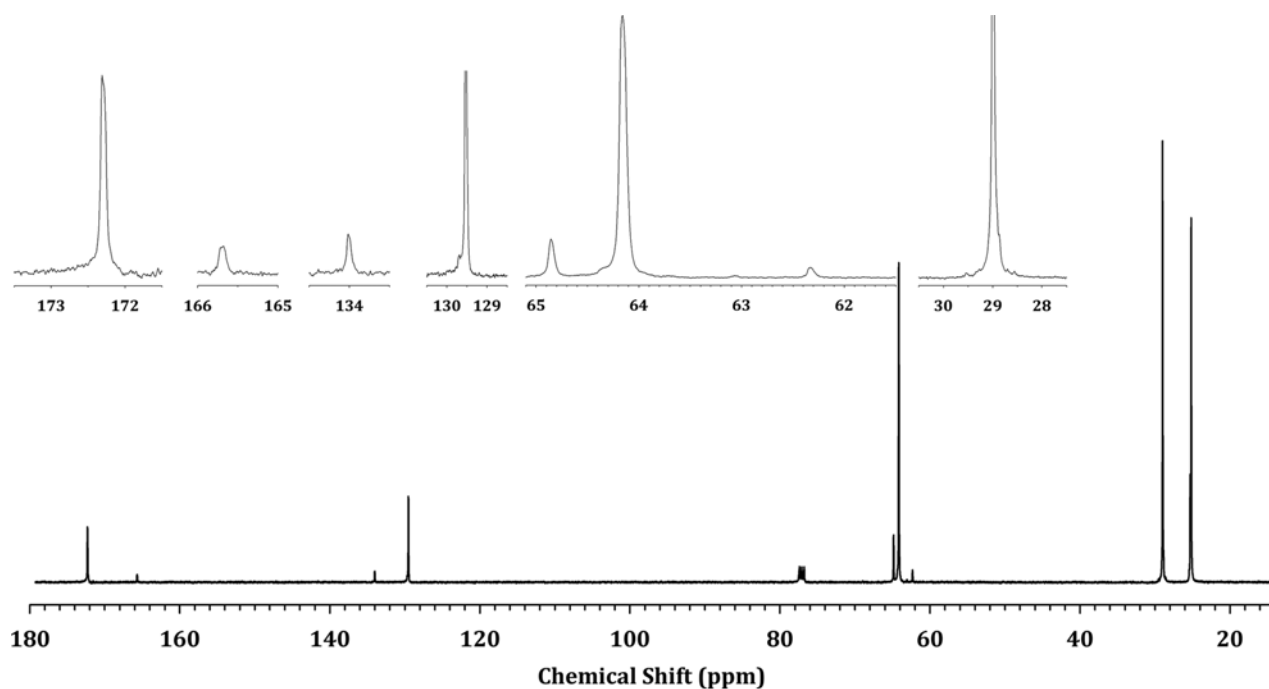


Figure 3. ^{13}C NMR spectrum of PBSET10.

Figure 3 shows the ^{13}C NMR spectrum of PBSET10. Assignments for shifts are: $^{\text{B}}\text{C}_a$ (25.187 ppm), $^{\text{T}}\text{C}_a$ (165.680 ppm), $^{\text{T}}\text{C}_b$ (134.014 ppm), $^{\text{T}}\text{C}_c$ (129.529 ppm), $^{\text{S}}\text{H}_a$ (28.997 ppm), and $^{\text{S}}\text{H}_b$ (172.308 ppm).^{16,19,20} Subscripts are shown in the Scheme II. BG:EG and TPA/SA molar ratio in polymer chains was calculated according to the following equations:

$$\text{BG/EG} = \frac{^{\text{E}}\text{H}_a}{(^{\text{E}}\text{H}_a + ^{\text{B}}\text{H}_a)} \quad (14)$$

$$\text{TPA/SA} = \frac{^{\text{T}}\text{C}_a}{(^{\text{T}}\text{C}_a + ^{\text{S}}\text{C}_b)} \quad (15)$$

$$\text{TPA/SA} = \frac{^{\text{T}}\text{C}_a}{2(^{\text{T}}\text{C}_c/2 + ^{\text{S}}\text{C}_a)} \quad (16)$$

The results are shown in Table II. As shown, TPA:SA molar ratio of feed and copolyesters is almost the same but EG mole percent in the final product is more than that of the feed. These results demonstrate that only end groups affect the polycondensation mechanism, so TPA:SA molar ratio of feed and product is same. In addition, there is a competition between hydroxyl ethyl and hydroxyl butyl, as end group, to evacuate during polycondensation and as can be seen, EG has more

reactivity than BG. Moreover, incorporation of BHET leads to the decrease in butylene succinate length and L_{nBS} decrease with BHET.

Figure 4 shows heating DSC thermograms of the samples.

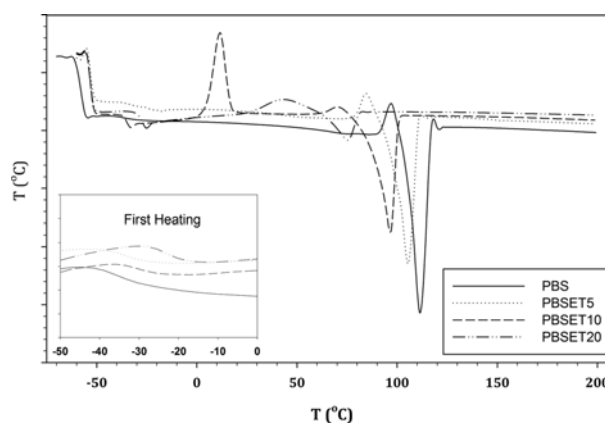


Figure 4. Heating DSC thermogram of PBS and its copolyesters.

Table II. H NMR and C NMR Result of Synthesized PBS and Its Copolyesters

Sample	Feed Ratio of BHET:BHBS	TA:SA ^a	EG:BG	TA:SA ^b	TA:SA ^c	L_{nET}	L_{nBT}	L_{nES}	L_{nBS}	B
PBS	0:100	0:100	0:100	0:100	0:100	0	0	0	-	0
PBSET5	5:95	4.9:95.1	6.3:93.7	4.9:95.1	5.8:94.2	1.47	1.46	1.64	39.04	0.73
PBSET10	10:90	9.4:90.6	13.1:86.9	10:90	12.4:87.6	1.62	1.59	1.80	17.77	0.73
PBSET20	20:80	19.2:80.8	24.9:75.1	19.9:80.1	23.7:76.3	1.98	2.12	2.35	4.19	0.79

^aReal TA:SA ratio calculated by ^1H NMR (eq. (4)). ^bReal TA:SA ratio calculated by ^{13}C NMR (eq. (15)). ^cReal TA:SA ratio calculated by ^{13}C NMR (eq. (16)).

Table III. DSC and XRD Data of Neat PBS and Its Copolyesters

Sample	T_g (°C)	T_c (°C)	ΔT_c (°C)	$\frac{\Delta H_c}{\text{Time}}$ (J/g)	ΔH_m (J/g)	T_m (°C)	ΔT (°C)	T_m (°C)	χ_c (%)	n	Z_l	L_{110} (nm)
PBS	-34.5	73.17	21.86	0.57	75.82	111.86	38.69	21.42	36.1	2.34	0.169	9.36
PBSET5	-32.2	50.77	32.62	0.35	70.97	105.49	54.72	23.42	33.8	2.23	0.073	5.12
PBSET10	-28.8	27.35	62.63	0.054	61.05	96.61	69.26	28.02	29.1	2.20	0.025	4.16
PBSET20	-22.6	-	-	-	12.73	75.54	-	29.54	6.1	2.16	0.023	3.45

Related data are given in Table III. As could be seen, copolyesters show a single glass transition between those of the PBS and PET homopolymers. The presence of BHET hard segment in the structure restricts the chain motion which leads to increase T_g . However, for all of the copolyesters, the negative deviation is observed from the Fox equation which indicates the decrease of intermolecular interactions.²¹ The thermogram of neat PBS shows a relatively sharp exothermal peak and a melting point at 116 °C. The melting temperature decreases with introducing comonomer to the polymer and the exothermal peak broadens and shifts to lower temperatures. These results indicate that the incorporation of BHET leads to the change of crystallization behavior. Introducing BHET, which is structurally different from the PBS chain repeating unit, can be expected to alter its crystallization behavior. Obviously, the type and concentration of the comonomer is important. Two possibilities exist with respect to the disposition of the comonomer. In one case, the crystalline phase remains pure and the comonomers are excluded from entering the crystal lattice. In the other case, the comonomer is allowed to enter the lattice.²² When the crystalline phase only contains the major monomer and remains pure, the Baur's equation for a random ideal copolymer is correct:²³

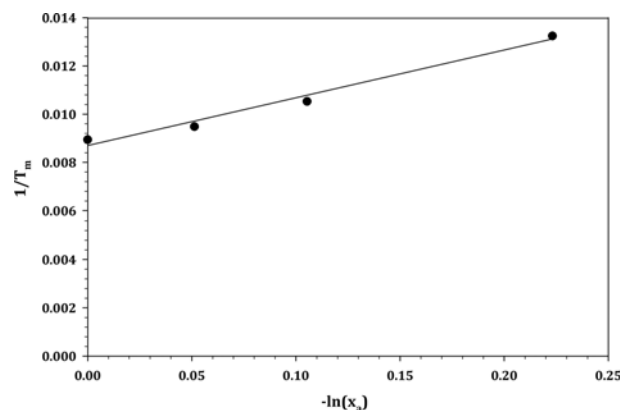
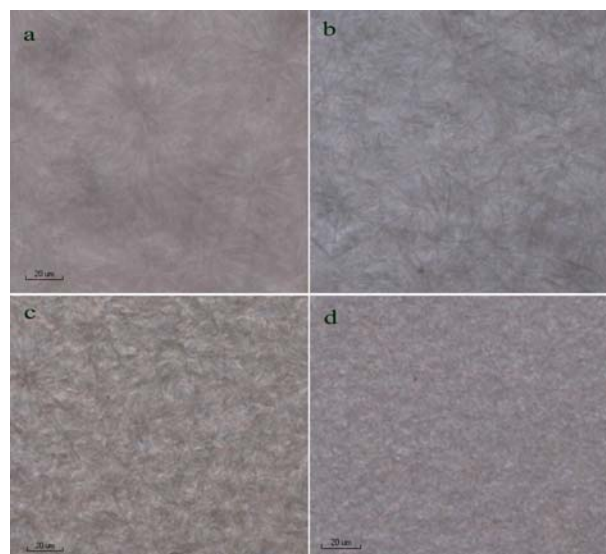
$$\frac{1}{T_m} - \frac{1}{T_m^0} = -\frac{R}{\Delta H_u} \ln(x_a) \quad (17)$$

where T_m , T_m^0 , R , ΔH_u , x_a are the melting temperature, equilibrium melting temperature, gas constant, enthalpy of fusion and main monomer composition, respectively. Figure 5 shows the plot of $1/T_m$ versus $-\ln(x_a)$ and eq. (18) shows the fitting results, which indicate that the crystals of the resulted copolyesters only contain BHBS unit and BHET excluded from the lattice.

$$\frac{1}{T_m} = -0.0196 \ln(x_a) + 0.0087, R^2 = 0.982 \quad (18)$$

¹H NMR results show that introduction of comonomer leads to reduce BHBS sequence lengths. Consequently, the size of crystallite decreases with the comonomer content. Figure 6 represents the optical micrographs of all copolyesters. The picture shows that incorporating comonomer reduces the crystal size however, increasing the nuclei per square meter and approved previous results.

In cooling, T_c is the temperature that the maximum overall

**Figure 5.** Plot of $1/T_m$ against $-\ln(x_a)$ for PBSET.**Figure 6.** Optical micrographs of (a) PBS, (b) PBSET5, (c) PBSET10, and (d) PBSET20.

crystallization rate is happened. Thus, the degree of supercooling ($\Delta T = T_m - T_c$) could be a measure of polymer crystallization ability: the greater the ΔT , the lower the overall crystallization rate.²⁴ ΔT values for the copolymer increase with the increase of ET content. These results confirm that overall crystallization rate for the copolymers are less than that of the neat PBS. It was observed that ΔT_m increases in copolymer, therefore, it could be concluded that the distribution

of crystallite size in copolymer was broader than neat PBS and smaller crystallites are produced which then melt at the lower temperatures. A cold crystallization can be seen in PBSET10 curve at about 11 °C which shows that cooling rate is very quick. If a crystallizable polymer quickly cooled from the molten state, crystallinity could decrease with the cooling rate. When such materials are heated above their T_g , crystallization occurs at temperatures between T_g and T_m . This process is called cold crystallization. This result indicates that PBSET10 is crystallizable as PBS and PBSET5 but with a lower rate.

The degree of crystallinity (χ_c) of PBS and copolymers were calculated according to the following equation:

$$\chi_c = \left(\frac{\Delta H_m}{\Delta H_{m0}} \right) \times 100 \quad (19)$$

where ΔH_m is the measured heat of fusion, and ΔH_{m0} is the heat of fusion for 100% crystalline polymer. The heat of fusion for 100% crystalline PBS is 210 J/g.²⁵ As seen in Table III, there is no significant change in the degree of crystallinity with increasing ET content up to 10 wt% but it decreases sharply when 20 wt% of ET comonomer is used.

Figure 7 displays WAXD patterns of PBS and its copolyesters that were cooled from 120 °C to room temperature and crystallized non-isothermally. The unit cell of the crystalline PBS α form is monoclinic,^{26,27} and the diffraction peaks from the (020) and (110) planes are detected at $2\theta \approx 19.6$ and 22.6° , respectively. All copolyesters have diffraction peaks of the PBS α form, revealing only one crystalline form. As

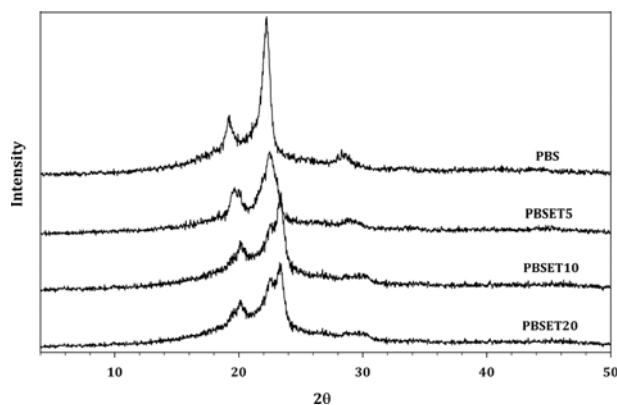


Figure 7. Wide-angle X-ray diffraction patterns of PBS and its copolyesters.

the proportion of the BHET units increases, the intensity of the diffraction peaks from the (020) and (110) planes becomes weaker and the width at half maximum peak increases gradually. The mean crystal sizes L_{hkl} , perpendicular to the (hkl) plane, could be estimated with the Scherrer equation:²⁸

$$L_{hkl} = \frac{K\lambda}{B\cos(\theta)} \quad (20)$$

where B is the width at half-maximum peak corrected for instrumental broadening and K denotes the Scherrer factor (0.9). L_{hkl} was strongly dependent on the peak broadening (B). The result is summarized in Table III. Figure 7 shows that the crystallite sizes declines with increasing the BHET content, indicating less crystalline order in copolymers and confirmed previous results of DSC and optical micrographs.

Cooling DSC curves (Figure 8) show that T_c of copolyesters is lower than T_c of PBS. Changes in crystallization peak width (ΔT_c) and ΔH_c are related to the overall crystallization rate and degree of crystallization, respectively.²⁹ The ΔT_c values for copolymer, that are 11–40 °C, are more than those for PBS (21.86 °C), and PBSET20 exhibited zero ΔT_c . Crystallization rates are defined as heat of crystallization divided by time from onset up to completion of crystallization ($\Delta H_c/\text{time}$). As seen in Table III, the values of $\Delta H_c/\text{time}$ for copolymer are lower than those of neat PBS (0.57 J/g s). In other words, the crystallization rates for the copolymer are less than PBS.

Non-isothermal crystallization of polymers could be studied by replacing t in avrami equation with T/C which is called Ozawa equation:^{23,30,31}

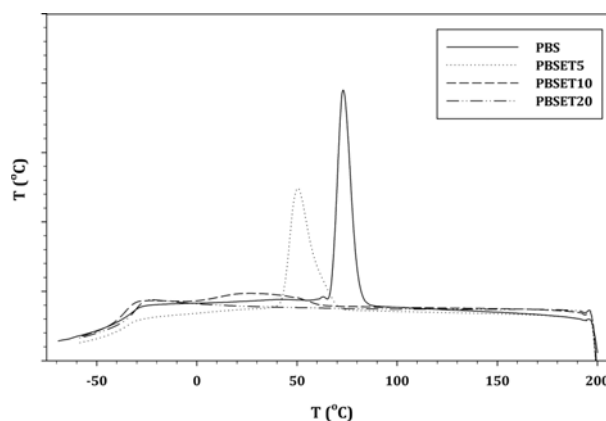


Figure 8. Cooling DSC thermogram of PBS and its copolyesters.

Table IV. DMA and Tensile Results of Synthesized PBS and Its Copolyesters

Sample	T_g	E (GPa)	Elongation @ break	E (MPa)	σ (MPa)
PBS	-11.57	2.97	10.93	668	38.8
PBSET5	-10.10	2.76	8.47	464	23.7
PBSET10	-7.71	2.88	587.26	412	27.7
PBSET20	-0.31	2.75	599.01	176	14.6

$$X_t = 1 - \exp(-Z_t t^n) \quad \& \quad t = \frac{T_0 - T}{C} \quad (21)$$

Or in double-logarithmic form:

$$\ln[-\ln(1-X_t)] = \ln Z_t + n \ln t \quad (22)$$

where n , Z_t , C , and X_t are Avrami constant which represents the mechanism of nucleation, Ozawa growth rate constant, cooling rate and relative crystallinity at the constant temperature at time t . The relative crystallinity (X_t) as a function of time is computed by the following equation:

$$X_t = \frac{\int_{t_0}^t (dH_c/dt) dt}{\int_{t_0}^{t_\infty} (dH_c/dt) dt} \quad (23)$$

where t_0 and t_∞ are the initial and end times of crystallization, respectively. Using DSC data, X_t was plotted versus t for all samples (Figure 9). It can be observed that all curves have similar shape and show the slower crystallization rate for copolymers. Figure 10 shows the double logarithm plots of $\ln[-\ln(1-X_t)]$ versus $\ln t$ for all samples. Slopes of these linear plots show Avrami exponent (n) and intercepts show Avrami growth rate constant (Z_t) which are listed in Table III. The range of n is from 2.16 up to 2.34 for PBS and copolymers which indicate that there are spherical crystals forms in copolymers.²¹ Z_t values are reduced with the amount of comonomer, confirming the decrease of crystallization rate. For neat PBS, crystal nucleus forms and molecular chains arrange rapidly at T_c but for the copolymer with heterogeneous nucleus, the nucleation type should be a heterogeneous one with a three-dimensional crystal growth.

Figure 11 gives DMA results of PBS and its copolyesters. Table IV presents the quantitative results of storage modulus (E) and $\tan\delta$. As mentioned before, copolyesters show a

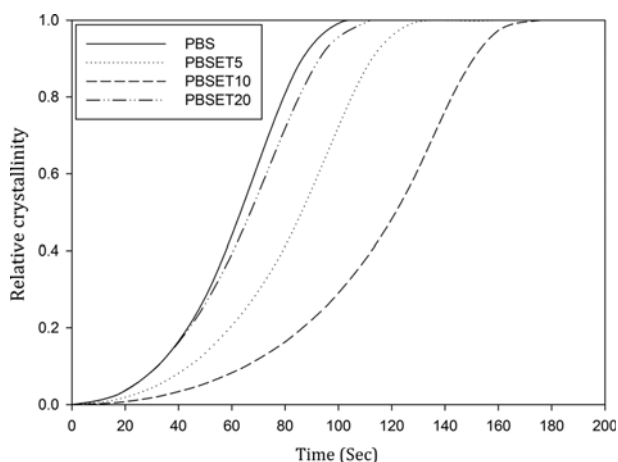


Figure 9. Development of X_t with t for non-isothermal crystallization of PBS and its copolyesters.

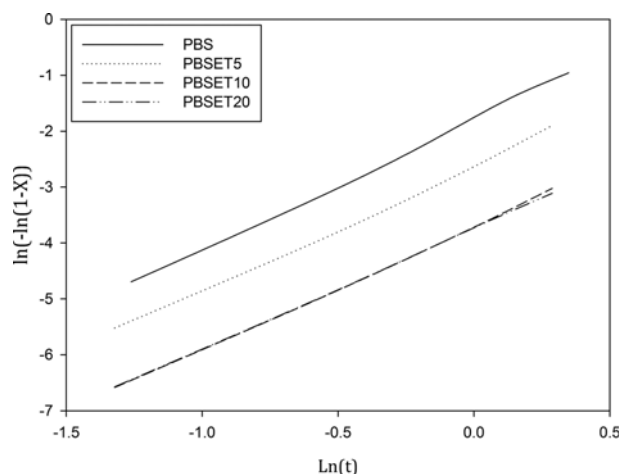


Figure 10. Plots of $\ln[-\ln(1-X_t)]$ versus $\ln t$ for all samples.

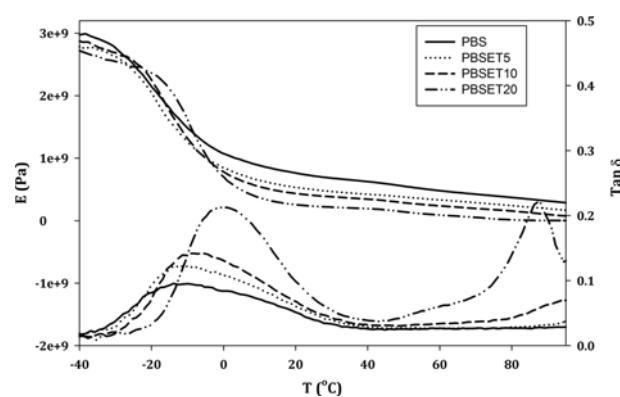


Figure 11. DMTA result of PBS and its copolyesters.

single glass transition between those of the PBS and PET homopolymers due to the introduction of hard segment to the structure. Moreover, the relaxation broadens with the increases of crystallinity, and the loss peak shifts to the higher temperatures.²¹ The results show that the copolyester with the comonomer content up to 10% has relatively the same crystallinity but PBSET20 crystallinity is much smaller than that which approved DSC results. PBSET20 shows another peak at 83 °C which is related to the melting temperature and it is the same as DSC result. Storage modulus curves show a slight decrease at the ambient temperature with the aromatic comonomer content. Thus, a polymer shows higher modulus if it has the higher crystallization degree or owns hard segment.^{32,33} As previously shown, incorporation BHET leads to decrease in crystallinity. So, there is a competition between decreasing crystallinity and increasing soft segment content on changing storage modulus. DMTA results show that the presence of hard segment up to 10% can prevent the decrease of modulus with crystallinity. Moreover, elongation at break (Figure 12) increases dramatically with BHET addition. Numerous, small and imperfect crystallites lead to an increase in the

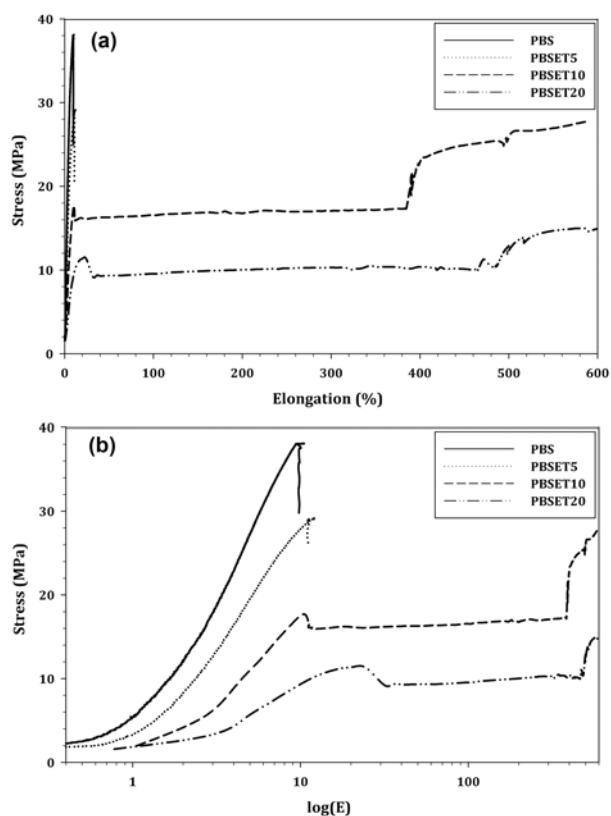


Figure 12. Tensile test result of PBS and its copolyesters.

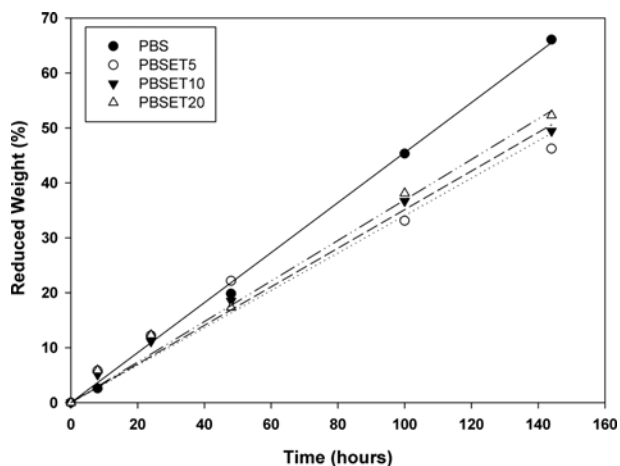


Figure 13. Hydrolytic degradation of PBS and its copolyesters.

impact strength and the elongation at break increases,³⁴ and as seen earlier, PBSET copolymer has lower crystallite size due to incorporating BHET which leads to increase in elongation at break up to 500%.

In vitro accelerated degradation of copolyesters was evaluated using NaOH solution at 37 °C. The results were shown in Figure 13 and Table V. Hydrolytic degradation is the scissoring of ester group by water which is affected by its chemical

Table V. Hydrolytic Degradation of PBS and Its Copolyesters

	PBS	PBSET5	PBSET10	PBSET20
k (1/h)	0.455	0.340	0.351	0.369
R^2	0.998	0.949	0.989	0.982
$t_{1/2}$ (h)	109.9	147.1	142.5	135.5

structure and surrounding biological environment. First, the water diffuses into the polymer, polymer chain scission happens, and then mass-loss occurs due to the removal of resulted oligomers.³⁵ The diffusion rate of water and by-products may be neglected using thin-film as sample, so the kinetics of the hydrolysis can be described by the following equation:

$$w = kt \quad (24)$$

where w , k , and t are the percentage of weight loss, rate constant and time, respectively. In the Table V, $t_{1/2}$ is reported, too. The $t_{1/2}$ is the time that half of the polymer is degraded.

As it can be seen, incorporating BHET into the main chain despite literature^{10,36,37} has no considerable effect on hydrolytic degradability. The hydrolytic rate increases with the number of hydrolysable groups, low crystallinity, hydrophilicity, absence of cross-links and the surface area of the material.³⁵ It is expected that the presence of aromatic group brings about reduce in degradability but decrease in crystallinity and crystallite size, as mentioned in DSC and DMTA results, leads to an increase in degradability. Consequently, copolymerization has a little effect on degradability.

Conclusions

A series of PBSET copolyesters were synthesized by polycondensation of BHET and BHBS, produced by esterification of 1,4-butanediol, ethylene glycol, succinic acid and terephthalic acid. The resulted copolyesters show improved properties in comparison to the neat PBS. As expected, the introduction of BHET hard segment causes a decrease in the crystallinity degree and melting point, due to a decrement of chain symmetry and regularity, and increase of the glass transition temperature, because of the presence of hard segment. NMRs results show that the higher the mol% of comonomer, the lower the PBS sequence length with a random distribution. Crystal morphology was investigated using Baur and Ozawa equations which indicate that only PBS is present in crystallite and there are spherical crystal forms in all copolyesters. Investigation of the mechanical properties show a slight decrease in the elastic modulus and a dramatically increase in the elongation at break up to 500% due to decrease in crystallite and crystallinity. The hydrolytic biodegradation rate of copolyesters, despite previous publications, slightly decreases with aromatic comonomer due to reducing crystallite size and crystallinity.

References

- (1) V. N. Vasilets, V. A. Surguchenko, A. S. Ponomareva, E. A. Nemetz, V. I. Sevastianov, J. W. Bae, and K. D. Park, *Macromol. Res.*, **23**, 205 (2015).
- (2) C. W. Lee, Y. Kimura, and J. D. Chung, *Macromol. Res.*, **16**, 651 (2008).
- (3) M. A. Hillmyer and W. B. Tolman, *Acc. Chem. Res.*, **47**, 2390 (2014).
- (4) A. Díaz, L. Franco, F. Estrany, L. J. del Valle, and J. Puiggali, *Polym. Degrad. Stab.*, **99**, 80 (2014).
- (5) Y. Zhao and Z. Qiu, *Macromol. Res.*, **22**, 693 (2014).
- (6) D. G. Papageorgiou, K. Chrissafis, E. Pavlidou, E. A. Deliyanni, G. Z. Papageorgiou, Z. Terzopoulou, and D. N. Bikiaris, *Thermochim. Acta*, **590**, 181 (2014).
- (7) B. Laycocka, P. Halleya, S. Pratt, A. Werker, and P. Lant, *Prog. Polym. Sci.*, **38**, 536 (2013).
- (8) D. N. Bikiaris and D. S. Achilias, *Polymer*, **49**, 3677 (2008).
- (9) V. Tserki, P. Matzinos, E. Pavlidou and C. Panayiotou, *Polym. Degrad. Stab.*, **91**, 377 (2006).
- (10) D. P. R. Kint, A. Alla, E. Deloret, J. L. Campos, and S. Munoz-Guerra, *Polymer*, **44**, 1321 (2003).
- (11) M. Wojtczak, S. Dutkiewicz, A. Galeski, and E. Piorkowska, *Eur. Polym. J.*, **55**, 86 (2014).
- (12) M. Kowalczyk, E. Piorkowska, S. Dutkiewicz, and P. Sowinski, *Eur. Polym. J.*, **59**, 59 (2014).
- (13) B. Stuart, *Infrared Spectroscopy: Fundamentals and Applications*, Wiley, Chichester, 2004.
- (14) Y. K. Han, S. R. Kim, and J. Kim, *Macromol. Res.*, **10**, 108 (2002).
- (15) F. Q. Kondratowicz and R. Ukielski, *Polym. Degrad. Stab.*, **94**, 375 (2009).
- (16) S. Velmathi, R. Nagahata, J. I. Sugiyama, and K. Takeuchi, *Macromol. Rapid. Comm.*, **26**, 1163 (2005).
- (17) R. S. Loup, T. Jeanmaire, J. J. Robin, and B. Boutevin, *Polymer*, **44**, 3437 (2003).
- (18) C. H. Chen, H. Y. Lu, M. Chen, J. S. Peng, C. J. Tsai, and C. S. Yang, *J. Appl. Polym. Sci.*, **111**, 1433 (2009).
- (19) Y. Zhang, Z. Feng, Q. Feng, and F. Cui, *Eur. Polym. J.*, **40**, 1297 (2004).
- (20) E. Olewnik, W. Czerwinski, J. Nowaczyk, M. O. Sepulchre, M. Tessier, S. Salhi, and A. Fradet, *Eur. Polym. J.*, **43**, 1009 (2007).
- (21) J. D. Menczel and R. B. Prime, in *Thermal Analysis of Polymers: Fundamentals and Applications*, Wiley, Hoboken, 2009, Chap. 2.
- (22) Z. Gan, H. Abe, H. Kurokawa, and Y. Doi, *Biomacromolecules*, **2**, 605 (2001).
- (23) L. Mandelkern, in *Crystallization of Polymers: Equilibrium Concepts*, Cambridge University Press, Cambridge, 2002, Chap. 5.
- (24) S. Y. Hwang, A. A. Khaydarov, J. Y. Park, E. Yoo, and S. S. Im, *Macromol. Res.*, **19**, 699 (2011).
- (25) G. Z. Papageorgiou, D. G. Papageorgiou, K. Chrissafis, D. Bikiaris, J. Will, A. Hoppe, J. A. Roether, and A. R. Boccaccini, *Ind. Eng. Chem. Res.*, **53**, 678 (2014).
- (26) Y. Ichikawaa, H. Kondoa, Y. Igarashia, K. Noguchia, K. Okuyamaa, and J. Washiyama, *Polymer*, **41**, 4719 (2000).
- (27) J. Zhang, X. Wang, F. Li, and J. Yu, *Fibers and Polymers*, **13**, 1233 (2012).
- (28) K. M. Choi, S. W. Lim, M. C. Choi, D. H. Han, and C. S. Ha, *Macromol. Res.*, **22**, 1312 (2014).
- (29) C. F. Ou, *J. Polym. Sci. Part B: Polym. Phys.*, **41**, 2902 (2003).
- (30) S. N. Sheikholeslami, M. Rafizadeh, F. A. Taromi, and H. Bouhendi, *J. Thermoplastic Comp. Mater.*, **27**, 1530 (2014).
- (31) Y. Wang, W. Liu, and H. Zhang, *Polym. Test.*, **28**, 402 (2009).
- (32) S. Fakirov, in *Handbook of Condensation Thermoplastic Elastomers*, Wiley-VCH, Weinheim, 2005, Chap. 3.
- (33) Y. Srithep, P. Nealey, and L. S. Turng, *Polym. Eng. Sci.*, **53**, 580 (2013).
- (34) A. El-Hadi, R. Schnabel, E. Straube, G. Muller, and S. Henning, *Polym. Test.*, **21**, 665 (2002).
- (35) F. Buchanan, *Degradation Rate of Bioresorbable Materials Prediction and Evaluation*, Woodhead Publishing Limited, Boca Raton, 2008, Chap. 3 & 9.
- (36) Q. Y. Zhu, Y. S. He, J. B. Zeng, Q. Huang, and Y. Z. Wang, *Mater. Chem. Phys.*, **130**, 943 (2011).
- (37) J. Xu and B. H. Guo, *Biotechnol. J.*, **5**, 1149 (2010).